Biogeosciences, 21, 4395–4411, 2024
https://doi.org/10.5194/bg-21-4395-2024

Biogeosciences Open Access EGU

Diverse organic carbon dynamics captured by radiocarbon analysis of distinct compound classes in a grassland soil

Katherine E. Grant[1], Marisa N. Repasch[1,2,3], Kari M. Finstad[1], Julia D. Kerr[1], Maxwell Marple[1], Christopher J. Larson[1,4], Taylor A. B. Broek[1], Jennifer Pett-Ridge[1,5], and Karis J. McFarlane[1]

[1]Physical and Life Sciences Directorate, Lawrence Livermore National Laboratory, Livermore, CA 94550, USA
[2]Institute of Arctic and Alpine Research, University of Colorado, Boulder, CO, USA
[3]Earth and Planetary Sciences, University of New Mexico, Albuquerque, NM, USA
[4]Department of Earth and Environmental Science, University of Pennsylvania, Philadelphia, PA, USA
[5]Life and Environmental Sciences Department, University of California-Merced, Merced, CA, USA

Correspondence: Katherine E. Grant (grant39@llnl.gov)

Received: 22 December 2023 – Discussion started: 8 January 2024
Revised: 7 August 2024 – Accepted: 11 August 2024 – Published: 10 October 2024

Abstract. Soil organic carbon (SOC) is a large, dynamic reservoir composed of a complex mixture of plant- and microbe-derived compounds with a wide distribution of cycling timescales and mechanisms. The distinct residence times of individual carbon components within this reservoir depend on a combination of factors, including compound reactivity, mineral association, and climate conditions. To better constrain SOC dynamics, bulk radiocarbon measurements are commonly used to trace biosphere inputs into soils and to estimate timescales of SOC cycling. However, understanding the mechanisms driving the persistence of organic compounds in bulk soil requires analyses of SOC pools that can be linked to plant sources and microbial transformation processes. Here, we adapt approaches, previously developed for marine sediments, to isolate organic compound classes from soils for radiocarbon (^{14}C) analysis. We apply these methods to a soil profile from an annual grassland in Hopland, California (USA), to assess changes in SOC persistence with depth (down to 1 m). We measured the radiocarbon values of water-extractable organic carbon (WEOC), total lipid extracts (TLEs), total hydrolyzable amino acids (AAs), and an acid-insoluble (AI) fraction from bulk and physically separated size fractions (< 2 mm, 2 mm–63 µm, and < 63 µm). Our results show that Δ^{14}C values of bulk soil, size fractions, and extracted compound classes became more depleted with depth, and individual SOC components have distinct age–depth distributions that suggest distinguishable cycling rates. We found that AAs and TLEs cycle faster than the bulk soils and the AI fraction. The AI was the most ^{14}C-depleted fraction, indicating that it is the most chemically inert in this soil. Our approach enables the isolation and measurement of SOC fractions that separate functionally distinct SOC pools that can cycle relatively quickly (e.g., plant and microbial residues) from more passive or inert SOC pools (associated with minerals or petrogenic) from bulk soils and soil physical fractions. With the effort to move beyond SOC bulk analysis, we find that compound class ^{14}C analysis can improve our understanding of SOC cycling and disentangle the physical and chemical factors driving OC cycling rates and persistence.

1 Introduction

Soil organic carbon (SOC) is a large and complex terrestrial reservoir of Earth's organic carbon (OC) (Jobbágy and Jackson, 2000). It is a highly dynamic and open pool with inputs from decaying plant material, living roots, and soil microbes and with losses driven by microbial activity that includes the degradation and transformation of compounds (Angst et al., 2021). The result of these processes is a heterogenous mixture of organic compounds with different radiocarbon (^{14}C) ages and reactivities (Lehmann and Kleber, 2015; Shi et al., 2020; Trumbore and Harden, 1997; Gaudinski et al., 2000; McFarlane et al., 2013). This complexity obscures the mechanisms that control overall OC persistence in soils, resulting

in a continued debate over the degree to which environmental factors, physical protection, and chemical composition influence SOC reactivity and persistence (Lützow et al., 2006; Lehmann et al., 2020; Schmidt et al., 2011).

Bulk analysis methods do not satisfactorily demonstrate how physical protection and chemical composition interact to influence SOC persistence, and so novel organic matter characterization methods can shed light on how different compound classes of OC are preserved in soils and through what mechanisms. For example, we need to understand how the chemical structure of OC influences interactions with mineral surfaces, such as aggregation or sorption, as well as how the environment influences the decomposition and resource availability of certain OC compounds and functional groups (Lehmann and Kleber, 2015; Schmidt et al., 2011; Kleber et al., 2021). However, it has been difficult to isolate, identify, and quantify pools of OC without altering OC molecular chemistry (Von Lutzow et al., 2007). Thus, specific organic compounds isolated from soils, such as amino acids and lipids (Rethemeyer et al., 2004), can provide information on how OC is stabilized in different environments. Therefore, multiple approaches, such as a physical separation followed by a chemical separation, are needed to fully understand the interplay between chemical compound reactivity and how carbon–mineral interactions function as part of SOC persistence in soil.

One approach used to investigate the controls on SOC persistence is to separate soil into operationally defined carbon pools (e.g., size or density fractions) and to characterize the resulting fractions. This approach has demonstrated that the association of OC with soil minerals is a critical mechanism for C stabilization (Vogel et al., 2014; Mikutta et al., 2007) as ^{14}C data indicate that some mineral-associated C can persist for thousands of years (Torn et al., 2009). However, ^{13}C-labeling experiments show that some mineral-associated C cycles quickly, within months to years (Keiluweit et al., 2015; De Troyer et al., 2011). Some biomolecules form strong associations with mineral surfaces, such as long-chain lipids with iron oxides (Grant et al., 2022), while other compounds only loosely associate with minerals such as through hydrophobic interactions with other OC compounds (Kleber et al., 2007). Therefore, physically isolated mineral-associated OC is still a heterogenous mixture of OC molecules that have a distribution of turnover times rather than a single homogenous and intrinsically stable SOC pool (Stoner et al., 2023; Van Der Voort et al., 2017).

Another approach that can yield finer resolution of OC turnover than traditional techniques is to isolate and measure the isotopic signature of specific compounds (Von Lutzow et al., 2007). In marine, riverine, and lacustrine systems, compound-specific radiocarbon analysis (CSRA) has been used to monitor the degradation of organic carbon through the marine water column (Loh et al., 2004), characterize marine particulate OC (Hwang and Druffel, 2003), constrain terrestrial OC burial and export from river systems (Galy et al., 2008, 2015; Repasch et al., 2021, Smittenberg et al., 2004), and determine the effect of OC export and burial on precipitation patterns and climate (Hein et al., 2020; Eglinton et al., 2021). Different types of compounds, including plant or microbial lipid biomarkers (Douglas et al., 2018; Huang et al., 1996), amino acids (Bour et al., 2016; Blattmann et al., 2020), lignin (Feng et al., 2013, 2017), certain carbohydrate compounds (Kuzyakov et al., 2014; Gleixner, 2013), and pyrogenic or black carbon (Coppola et al., 2018), can be isolated and analyzed for ^{14}C, leading to a more detailed understanding of the cycling of targeted compounds in the environment.

Each of these specific compounds can provide information related to the persistence, source, and potential fate of OC in soils. For instance, lipids are found in plant cell walls and microbial cell membranes and are used for energy storage. Amino acids are necessary for protein formation, are enriched in nitrogen relative to other plant and microbial residues, and likely play an important role in nitrogen mining and recycling. These two compound classes have diverse chemical reactivities, which allows for insight into chemical compound persistence. Understanding the abundance and age of these two biomarkers in soils can help differentiate the source of C used by soil microbes for metabolism and growth (e.g., new C inputs vs. older, recycled soil C), as well as the transformation pathways that yield persistent SOC.

Recently, CSRA approaches developed for these environments have been applied to soil, showing promise for identifying the distinct ages of plant and microbial biomarkers in SOC (Gies et al., 2021; Grant et al., 2022; Van Der Voort et al., 2017; Jia et al., 2023; Douglas et al., 2018). Most of these CSRA studies applied to SOC have targeted specific, individual biomarkers in soils, which generally contribute less than 5 % to the entire carbon pool (Lützow et al., 2006; Kögel-Knabner, 2002). This approach can be too specific to elucidate holistic mechanisms for SOC persistence and turnover that pertain to the majority of SOC. While individual biomarker ages, such as single ages of a particular lipid or single amino acid, can be useful in some contexts, comprehensive understanding of carbon compound class persistence is vital for understanding and modeling the vulnerability of soil carbon to degradation.

To strike a balance between too specific and too broad, some researchers have characterized broader compound classes rather than isolating a single biomarker. For example, this ^{14}C compound class approach has been applied to marine dissolved and particulate OC with a range of compounds, such as total lipids and total amino acids, to provide a broader understanding of OC persistence in oceans (Wang et al., 1998, 2006; Wang and Druffel, 2001; Loh et al., 2004). Wang et al. (1998) established a sequential extraction procedure to analyze ^{14}C abundance of total lipids, amino acids, carbohydrates, and a residual acid insoluble fraction from marine POC and sediments. This approach yielded distinct differences in the ^{14}C age and abundance of the amino

acids and lipids, in the acid-insoluble fraction in POC from the marine water column and sediment, and in coastal versus open-ocean environments. Loh et al. (2004) found the lipid fraction of dissolved OC and POC to be the oldest fraction measured in both the Atlantic and Pacific oceans, while the acid-insoluble fraction was intermediate in age, and the amino acids and carbohydrates contained a significant contribution of modern carbon. Wang and Druffel (2001) also used this approach and found that the lipids were the oldest compound class from sediments in the Southern Ocean, but the acid-insoluble residue was very similar in age to the lipid fraction. These studies suggest that compound classes can have independent cycling rates, but these cycling rates can be influenced by the environment.

Here, we apply a ^{14}C compound class approach to soils to more broadly understand SOC turnover mechanisms. We characterize the distribution and ^{14}C age of multiple SOC pools with depth in a well-studied annual grassland in California using soil physical fractionation (McFarlane et al., 2013; Poeplau et al., 2018) and modified compound class extraction methods previously detailed for marine sediments (Wang et al., 1998). We measured the radiocarbon values of water-extractable organic carbon (WEOC), total lipid extracts (TLEs), total hydrolyzable amino acids (AAs), and an acid-insoluble (AI) fraction from bulk and physically separated size fractions (bulk soil, sand, and silt + clay). We expected the TLE to be older than its source fraction (bulk soil, sand, or silt + clay), to be older with depth as the decline in plant inputs necessitates the recycling and use of older SOC, and to be older in the silt + clay fraction as its high surface area should result in mineral–OC associations that protect SOC from soil microbes (Grant et al., 2022; Van der vort et al., 2017). We expected the AAs to be younger than the TLE fraction and the bulk SOC pool based on the young ^{14}C ages found for AA extracted from marine sediments (Wang et al., 1998; Wang and Druffel, 2001), but we hypothesized that the recycling of amino acids at depth by soil microbes might result in an increase in the age of AAs below 50 cm. Finally, we expected AI to have old C, similarly to the TLE, as seen in marine sediments (Wang et al., 1998). Here, we describe the relative abundance and radiocarbon content of WEOC, total lipid, amino acid, and acid-insoluble compound class extracts in bulk soils and compare carbon storage and cycling rates within soil size fractions. These data provide a foundation for the continued application of compound class ^{14}C work to the understanding and modeling of soil OC persistence.

2 Materials and methods

2.1 Site and sample description

Soil samples were collected from the University of California's Hopland Research and Extension Center (HREC) in January 2022. The site is an annual grassland with a Mediterranean-type climate, where the mean annual precipitation (MAP) is 940 mm per year and the mean annual temperature is 15 °C (Nuccio et al., 2016). The underlying geology consists of mixed sedimentary rock of the Franciscan formation. The soils are designated as Typic Haploxeralfs of the Witherall-Squawrock complex (Soil Survey Staff, 2022). The samples were collected from the Buck site (39.001°, −123.069°), where the vegetation is dominated by annual wild oat grass, *Avena barbata* (Kotanen, 2004; Bartolome et al., 2007). Soils were collected from a freshly dug soil pit at four depths: 0–10, 10–20, 20–50, and 50–100 cm. The site is dominated by annual grasses, shallow rooted herbs, and forbs, and we did not observe roots below 10 cm. Thus, root-derived inputs of OC are important near the soil surface but do not directly affect deeper soils at this site. Samples were stored in sealed plastic bags at ambient temperature and transported to the laboratory in Livermore, CA. Soil samples were air dried, homogenized, and sieved to 2 mm, with the > 2 mm fraction retained for further analysis. Samples were subdivided for soil characterization, physical size separations, chemical compound extractions, and density fractionation.

2.2 Physical fractionation

To compare compound classes between mineral-associated OC and mineral-free OC, we used a salt-free and chemical-free method for isolating the mineral-associated organic matter from the free particulate organic matter (Fig. 1a). Under the assumption that mineral-associated carbon is primarily found in the silt + clay (< 63 µm) particle size fraction, we used a size fractionation sieving method where air-dried samples were dry-sieved into three size fractions: bulk soil (< 2 mm), sand (2 mm–63 µm), and silt + clay (< 63 µm) (Lavallee et al., 2020; Poeplau et al., 2018). Additionally, because the majority of free particulate organic carbon (POC) is contained in the sand faction, we used a "water density" separation to remove the low-density POC from the mineral matter in this fraction by suspending the sand fraction in 18.2 MΩ and removing the floating OC, resulting in a POC (< 1 g mL^{-1}) fraction and a POC-free (> 1 g mL^{-1}) sand fraction.

To further characterize these soils and aid in the interpretation of our data, we compared the size-fractionated samples to samples separated by density using sodium polytungstate (SPT-0 adjusted to a density of 1.65 g mL^{-1}) (Poeplau et al., 2018) (see Sect. S1.1 in the Supplement for detailed methods). We chose to focus our compound class extraction efforts on size-fractionated samples to avoid chemical alteration of SOC during exposure to SPT since SPT has a high ionic strength and low pH.

To constrain any contributions of OC from parent materials to SOC, we processed and analyzed the rock fraction (> 2 mm) (Agnelli et al., 2002; Trumbore and Zheng, 1996).

Rocks were washed with 18.2 MΩ water in an ultrasonic bath to remove surface contamination, rinsed with 1 N HCl to remove any additional weathered material loosely adhered to the surface, dried at 60°, and then manually crushed.

A large, representative aliquot (∼ 10 g) of the bulk and each physical fraction were ball milled and measured for total organic carbon (TOC, wt %), C/N ratio, $\delta^{13}C$, and $\Delta^{14}C$ (Sect. 2.6). In addition, we analyzed the bulk soils at each depth with nuclear magnetic resonance (^{13}C NMR) to assess the broad structural complexity of the OC in the bulk soil (Sect. S2).

2.3 Water-extractable organic carbon (WEOC)

The water-extractable organic carbon (WEOC) fraction was collected from 80 g of bulk soil with 18.2 MΩ water using a 4 : 1 water to soil ratio (Van Der Voort et al., 2019; Lechleitner et al., 2016; Hagedorn et al., 2004). Saturated soil samples were shaken for 1 h and then filtered through a pre-rinsed 0.45 µm polyethersulfone (PES) Supor filter under vacuum. An aliquot was taken for dissolved organic carbon (DOC) measurement on a Shimadzu TOC-L combustion catalytic oxidation instrument. Sample concentrations were determined using a nine-point DOC calibration curve ranging from 0 to 200 mgC L^{-1}. The WEOC fraction was dried using a Labconco CentriVap centrifugal drying system at 40 °C and subsequently transferred with 0.1 N HCl into pre-combusted quartz tubes to eliminate any inorganic carbon dissolved in the aqueous fraction. The acidified WEOC fractions were then dried down using the CentriVap. Dried samples were flame sealed under vacuum (Sect. 2.6) for subsequent carbon isotope analyses.

2.4 Total lipid extraction (TLE)

Total lipids were extracted from the soil samples using an accelerated solvent extraction (ASE) system (Dionex 350, Thermo Scientific) in duplicate. The total lipids were extracted from the bulk, sand, silt + clay, and the dense fraction (> 1.65 g mL^{-1}; DF). An aliquot of 10–30 g of soil was loaded into a stainless-steel ASE extraction cell depending on TOC content (Rethemeyer et al., 2004). The ASE was set to extract the sample for 5 min with a holding temperature of 100 °C at 1500 PSI. Lipids were extracted using a 9 : 1 ratio of dichloromethane (DCM or syn: methylene chloride) to methanol (Wang et al., 1998; Van Der Voort et al., 2017; Grant et al., 2022). The TLE was dried under constant ultrapure N_2 flow at 40° using a nitrogen dryer (Organomation MULTIVAP nitrogen evaporator). The TLE was resuspended in ∼ 5 mL of 9 : 1 DCM : methanol and then was transferred to pre-combusted quartz tubes, dried again, and analyzed for ^{14}C as described below (Sect. 2.5). Total CO_2 produced by the combustion of the TLE was measured manometrically on the ^{14}C vacuum lines during graphitization. Process blank samples were analyzed with each batch (Sect. S3.1).

2.5 Amino acid (AA) extraction

Amino acids (AAs) were extracted from the lipid-extracted residual bulk and silt + clay size fraction with an acid hydrolysis procedure, desalted, and isolated with cation exchange chromatography using methods modified from those used in marine systems (Wang et al., 1998; Ishikawa et al., 2018; Blattmann et al., 2020). Briefly, a 500 mg soil aliquot was hydrolyzed with 6N HCl (ACS grade) under an N_2 atmosphere for 19–24 h at 110 °C. After hydrolysis, amino acids in solution were separated from the solid acid-insoluble (AI) fraction via centrifugation for 5 min at 2500 rpm. The AI fraction was subsequently washed, at minimum, three additional times with 0.2 N HCl to ensure complete AA recovery. The supernatant was collected in a single pre-combusted vial and then filtered through a pre-combusted quartz wool fiber plug to remove extraneous sediment particles. The filtered hydrolysate was dried using a CentriVap at 60° for 4 h. The dried supernatant was redissolved in 1 mL 0.1 N HCl and loaded onto a preconditioned resin column (BioRad 50WX8 200–400 mesh resin) to isolate the AA from other hydrolyzed organic matter and to remove excess chloride. Details of the procedure can be found in Ishikawa et al., 2018. Briefly, once the sample was loaded onto the column, it was rinsed with three bed volumes (∼ 6 mL) of 18.2 MΩ H_2O. The free AAs were eluted with 10 mL of 2 N ammonium hydroxide (NH_4OH) and then were transferred into pre-baked quartz tubes, dried at 60° in the CentriVap, and finally sealed and combusted for isotopic analysis. The remaining rinsed solid residual after hydrolysis is the acid-insoluble (AI) fraction. These are processes constituting a solid sample for isotopic analysis.

2.6 Isotopic and elemental analysis

All samples were analyzed for radiocarbon (^{14}C) at the Center for Accelerator Mass Spectrometry (CAMS) at Lawrence Livermore National Lab (LLNL) in Livermore, California. Samples were either measured on a 10 MV Van de Graaff FN or a 1MV NEC compact accelerator mass spectrometer (AMS) (Broek et al., 2021), with average errors of $F^{14}C = 0.0035$. For solid-soil analysis, 10 to 250 mg of ground material was weighed into a pre-combusted quartz tube along with 200 mg CuO and Ag, flame sealed under vacuum, and then combusted at 900 °C for 5 h. The CO_2 was reduced to graphite on preconditioned iron powder under H_2 at 570° (Vogel et al., 1984). Measured ^{14}C values were corrected using $\delta^{13}C$ values and are reported as age-corrected $\Delta^{14}C$ values using the following the conventions of Stuiver and Polach (1977). Extraneous C was quantified for the TLE and AA extractions (Table S4 and Sect. S3). For ease of reference, we included conventional radiocarbon ages in our figures and tables. We quantified turnover times using the single-pool turnover model described in Sierra et al. (2014) and Van Der Voort et al. (2019) and explained in detail in

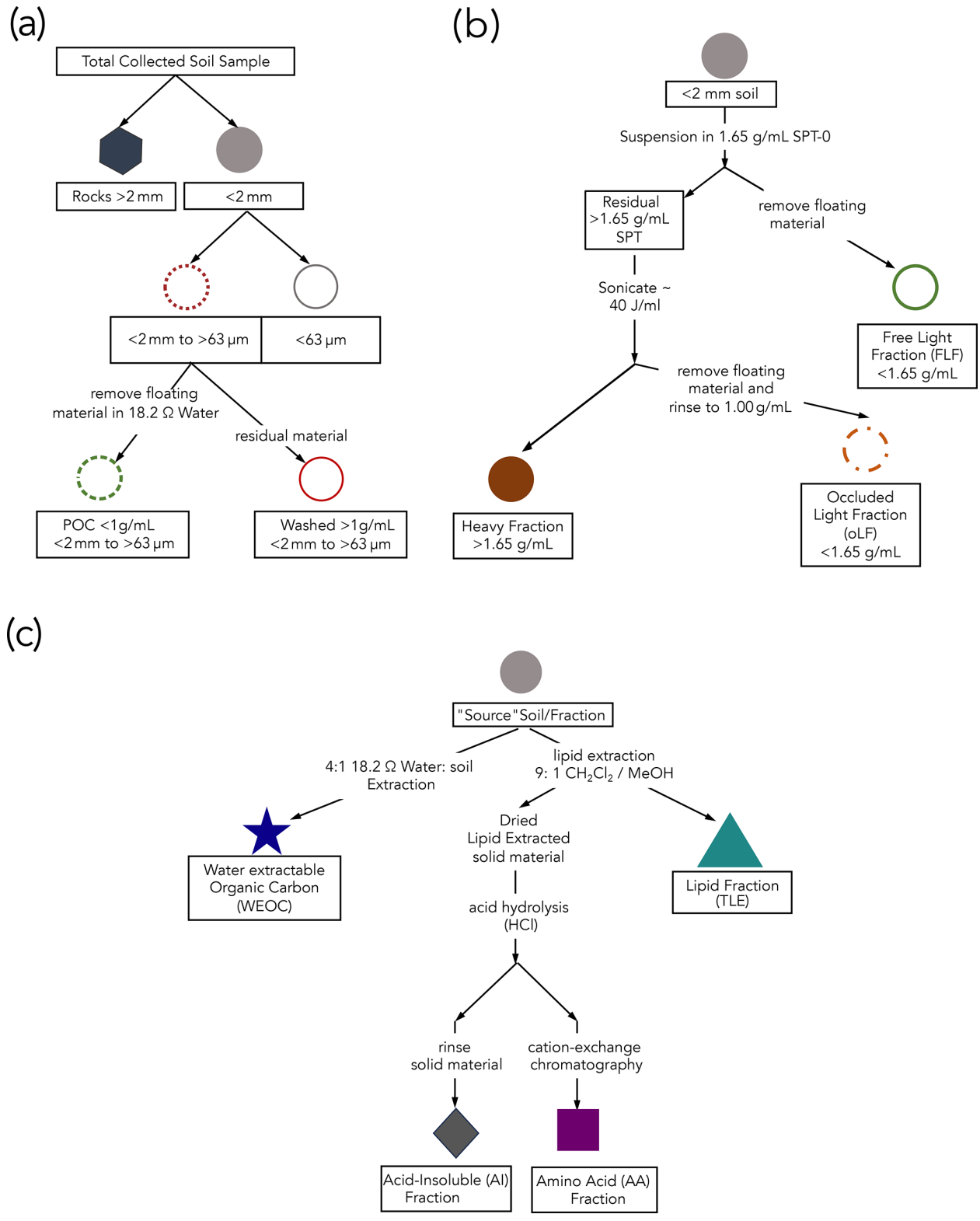

Figure 1. Schematics of protocols used in this study for **(a)** fractionation by size, **(b)** density separation (details in the Supplement), and **(c)** extraction of targeted compound classes. The "source soil/fraction" refers to the soil from which the different compound classes are extracted. All compound extractions and physical fractionations were applied to the < 2 mm bulk soil; total lipid extract (TLE), amino acid (AA), and acid-insoluble (AI) compound classes were also extracted from the silt + clay fraction, and only the TLE was extracted from the dense fraction (DF).

Trumbore (2000) and Torn et al. (2009). This approach generates two solutions for pools with $\Delta^{14}C > 0‰$, one corresponding to each side of the atmospheric ^{14}C–CO_2 curve over the last 70 years (Hua et al., 2022). Unfortunately, we cannot identify the correct solution (McFarlane et al., 2013; Trumbore, 2000), especially for TLE and AA fractions from the top 20 cm, as we do not have multiple time points or additional constraints such as pool-specific input or decomposition rates (see Sect. 2.8). Therefore, our data analysis and interpretations rely on the reported $\Delta^{14}C$ values. All individual ^{14}C measurements used in this study are listed in the Supplement (Tables S1 and S2).

For each solid sample, a dried homogenized aliquot was analyzed for TOC concentration and $\delta^{13}C$ using an elemental analyzer (CHNOS) coupled to an IsoPrime 100 isotope ratio mass spectrometer at the Center for Stable Isotope Biogeochemistry (CSIB) at the University of California, Berkeley. Samples are assumed to have no inorganic carbon based on acid-leaching tests and previously published ^{14}C work at this site (Finstad et al., 2023; Foley et al., 2023). $\delta^{13}C$ was measured in duplicate for each solid sample, and errors represent the standard deviation of the mean. $\delta^{13}C$ values of WEOC, TLE, and AA extracts were measured on a split of the cryogenically purified CO_2 and were analyzed at the Stable Isotope Geosciences Facility at Texas A&M University on a Thermo Scientific MAT 253 dual-inlet stable isotope ratio mass spectrometer (Table S1).

2.7 Data analysis

Data were analyzed using MATLAB version R20223 and R version 3.614 (R Core Team, 2021). Linear regressions were calculated between the sample depth mid-point and the $\Delta^{14}C$ values from both the size fractions, as well as between the extracted compounds (WEOC, TLE, AA, AI) from the different size fractions. This was done to directly compare the differences in $\Delta^{14}C$ values between the compound classes. Correlation coefficients, p values, and r^2 are provided in Table S3. Analysis of variance (ANOVA) was used to assess differences in $\Delta^{14}C$ with depth between TLE and AA and between soil fractions. ANOVA tests were performed in R version 3.614 (R Core Team, 2021). In the text, results are reported as means followed by 1 standard error when $n = 2$ or 3 or by analytical error when $n = 1$.

2.8 Interpretation of radiocarbon data

In the interpretation of soil ^{14}C activity, we must consider how ^{14}C created during the testing of atmospheric nuclear weapons may have affected the isotopic signatures of SOC at our study site. Significantly elevated "bomb-derived" ^{14}C was released into the environment during atmospheric nuclear weapons testing during the mid-20th century. This atmospheric radiocarbon spike has been continuously incorporated into carbon reservoirs, including vegetation, soils, and oceans (Levin and Hessshaimer, 2000). Plants assimilate CO_2 with the ^{14}C signature of the current year's atmosphere during photosynthesis and thus incorporate the current atmospheric ^{14}C signature into their tissues and root exudates. This signature then cycles into and through soils as this plant-derived organic matter decays, is processed by microbes, and enters stable soil organic matter pools (Torn et al. 2009). Since the termination of atmospheric weapon testing in the 1960s and with continued fossil fuel emissions, the ^{14}C of atmospheric CO_2 has decreased to approximately pre-1950 values, with $0 \pm 1‰$ being reported for the 2019 Northern Hemisphere growing season (Hua et al. 2022). Thus, soil carbon pools with ^{14}C signatures above $0‰$ can be interpreted as decadal-aged or decadal-cycling C, and pools with ^{14}C signatures below $0‰$ cycle on timescales of centuries to millennia.

3 Results

3.1 Radiocarbon values and characterization of the physical fractions

We used soil size and density fractionation to separate the bulk soil into fractions with different degrees of mineral protection. Radiocarbon content for the bulk soil, sand, and silt + clay (Table S3) became more ^{14}C-depleted (older) with increasing depth (Table 1, Fig. 2). SOC in the silt + clay was consistently younger than in the bulk soil, with the average difference in $\Delta^{14}C$ values increasing from $4‰$ at the surface to $87‰$ at depth. In the sand fraction, the $\Delta^{14}C$ values of POC were consistently near current atmospheric values ($2 \pm 3‰$) and were not significantly correlated with depth. In contrast, the $\Delta^{14}C$ values of the POC-free sand-sized fraction declined with depth ($25 \pm 3‰$ to $-510 \pm 2‰$, $p = 0.006$) and were indistinguishable from the POC-free sand fraction (Fig. 2). Density fractionation of the bulk soil resulted in most of the sample mass (> 98 %) and OC (75 %–83 %) recovered in the DF at all depths (Fig. S2).

3.2 Compound class results from bulk soil and silt + clay

In both the bulk soil and silt + clay fraction, the extracted compound classes became ^{14}C-depleted with depth, except for the WEOC, which had ^{14}C values that reflected C inputs recently fixed from the atmosphere throughout the soil profile (Fig. 2; tables in the Supplement). The $\Delta^{14}C$ values of the WEOC ranged from $14 \pm 4‰$ at the surface to $-46 \pm 4‰$ at depth, and the DOC concentrations ranged from 43.2 to 6.7 mg C g soil^{-1} at the surface and at depth, respectively.

The TLE from the bulk soil had $\Delta^{14}C$ values that range from $17 \pm 27‰$ to $-208 \pm 6‰$ ($n = 2$; ± SE) in the surface and deepest samples, respectively. In comparison, the TLE from the silt + clay fraction was modern at the surface and became more ^{14}C-depleted with depth ($p < 0.001$), from

Table 1. Carbon concentrations, mass fractions, and radiocarbon values for the size separations from the Buck pit.

	Bulk (< 2 mm)		Sand-sized (2 mm to 63 µm)			POC-free (> 1 g mL^{-1})		POC (< 1 g mL^{-1})		Silt + clay (< 63 µm)		
Depth	%OC	$\Delta^{14}C \pm$ err (‰)	mass f	%OC	$\Delta^{14}C \pm$ err (‰)	%OC	$\Delta^{14}C \pm$ err (‰)	%OC	$\Delta^{14}C \pm$ err (‰)	mass f	%OC	$\Delta^{14}C \pm$ err (‰)
0–10 cm	3.14	31 ± 3	0.71	2.68	25 ± 3	2.08	25 ± 3	25.69	19 ± 3	0.29	4.25	34 ± 3
10–20 cm	1.22	-22 ± 3	0.69	0.94	-38 ± 3	0.77	-35 ± 3	25.99	-5 ± 3	0.31	1.84	-13 ± 3
20–50 cm	0.50	-116 ± 3	0.75	0.39	-142 ± 3	0.38	-149 ± 2	n.m.	4 ± 3	0.25	0.85	-79 ± 3
50–100 cm	0.25	-468 ± 3	0.79	0.23	-496 ± 3	0.18	-510 ± 2	n.m.	-10 ± 3	0.21	0.35	-380 ± 3

46 ± 4 ‰ to -204 ± 36 ‰. The slopes of the linear regressions of $\Delta^{14}C$ with depth were indistinguishable in terms of TLE from the bulk soil and from silt + clay. In addition, the TLE from the bulk TLE and the silt + clay fraction TLE (tables in the Supplement) had very similar $\Delta^{14}C$ values, but the bulk soil had less lipid-C extracted during each experiment (280 µg g C^{-1} at 0–10 cm depth vs. 150 µg g C^{-1}; Table S2).

The $\Delta^{14}C$ values of the AAs extracted from the bulk soil ranged from 54 ± 5 to -183 ± 24 ($n = 2$, SE) with depth (Fig. 3, Table S3). Similarly, the $\Delta^{14}C$ value of the AA fraction extracted from silt + clay declined with depth from 60 ± 3 ‰ ($n = 2$, SE) at the surface to -106 ± 4 ‰ ($n = 2$, SE) at 50–100 cm depth. The slopes of the AAs extracted from the bulk and silt + clay size fractions were statistically different, indicating that the AAs extracted from the bulk soil became more depleted with depth than those extracted from the silt + clay (Table S3). Furthermore, AA fractions were enriched in ^{14}C relative to the TLE or AI fraction ($p < 0.01$ for bulk soil and $p < 0.05$ for silt + clay). The AI fraction was the oldest fraction found in our study at each depth. The $\Delta^{14}C$ values of the AI fraction ranged from -5 ± 2 ‰ to -633 ± 2 ‰ (analytical error, $n = 1$) and declined with depth ($p < 0.01$) for bulk soil and silt + clay (Fig. 3; Table S3).

4 Discussion

4.1 Variability of ^{14}C in compound classes in soils

We measured the radiocarbon content of four distinct soil chemical extracts: water-extractable organic carbon (WEOC), total lipid extract (TLE), free amino acids (AAs), and the acid-insoluble (AI) fraction, each of which had distinct $\Delta^{14}C$ values compared to the source soil they were extracted from (bulk or silt + clay; Fig. 4a and b). The central questions of this study are as follows: what are the differences in cycling time and/or age between various organic compounds in the soil? Do these differences in cycling time change with depth? As expected, $\Delta^{14}C$ values of TLEs, AAs, and AI became more depleted with depth (Fig. 3). More interestingly, the differences between the ^{14}C content of the source soil and the extracted compounds were not consistent with depth (Fig. 3a and b). This divergence in $\Delta^{14}C$ values reflects differences in turnover times among compound classes, which can be influenced by the sources of OC for each of these pools and by differences in the stabilization mechanisms protecting those compounds from decay. In this annual grassland, plant inputs should have a greater influence on SOC pools near the surface, which we confirmed with near-modern $\Delta^{14}C$ signatures in the 0–10 cm depth for all compound classes and size fractions (Fig. 3b and c). Furthermore, at deeper depths, new vegetation inputs should be less readily available, which results in more depleted $\Delta^{14}C$ signatures at depth and could necessitate microbial use and recycling of older SOC.

We found that, averaged across depths, the $\Delta^{14}C$ values of the TLEs were more depleted than those of the AAs, though both compound classes were more enriched in $\Delta^{14}C$ than the bulk soil or silt + clay from which they were extracted. The extracted AAs are the foundational units of hydrolyzed proteins and are found in both plant and microbial biomass (Blattmann et al., 2020). As in marine studies, we found the AAs to be the youngest compound class fraction (of the TLEs and AI) in these soils. The AA pool likely reflects a more actively cycling microbial pool, especially at depth, as AAs are enriched in nitrogen compounds, and it is likely that microbes both preferentially mine and recycle these compounds (Moe, 2013). The divergence from bulk ^{14}C values indicates that, even at depth in the soil, the AAs are either continuously replenished by the transport of AAs from surface horizons or re-synthesized with relatively ^{14}C-enriched sources such as the WEOC.

Based on published data for both soils and marine sediments, we expected the TLE to be older than both the AAs and the bulk soil; however, we found that all TLE samples, no matter what fraction we measured, were more ^{14}C enriched than the bulk soil. TLE is composed of a continuum of lipids from plant and microbial materials, ranging from leaf waxes to microbial cell structural components (Angst et al., 2016, 2021), that cycle at different rates and are likely to interact with mineral surfaces. Previous studies where individual lipid biomarker $\Delta^{14}C$ values were measured in soils on either short-chain or long-chain fatty acids found a divergence in $\Delta^{14}C$ values between these two pools, with short-chain lipids generally having enriched ^{14}C values and long-chain lipids having more depleted ^{14}C values (Grant et al., 2022; Van Der Voort et al., 2017). For example, long-chain lipid biomark-

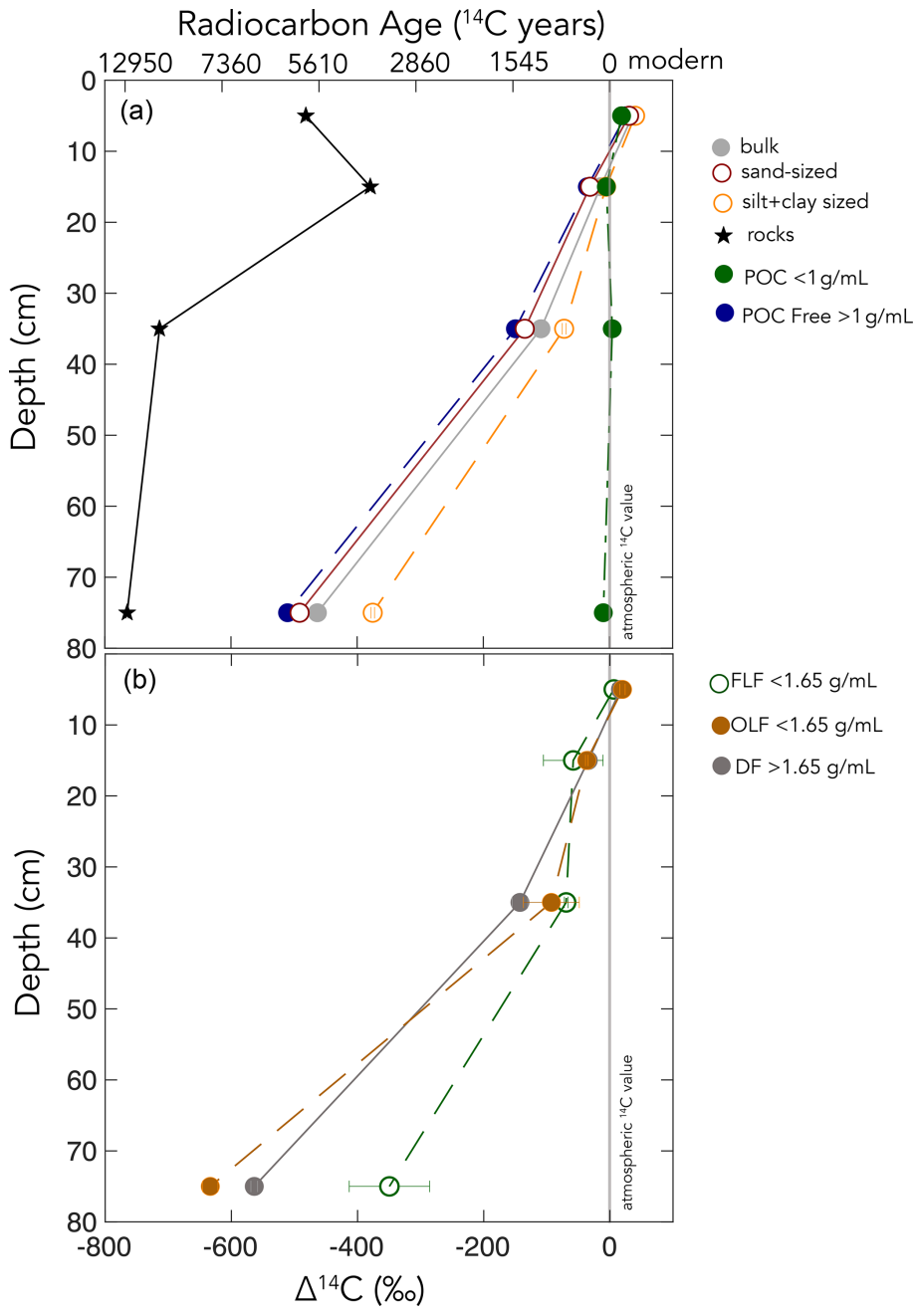

Figure 2. Δ^{14}C values by depth for **(a)** size fractions and **(b)** density fractions from the Buck soil pit. Conventional ^{14}C ages are provided for reference. The following abbreviations appear in the legend: particulate organic carbon (POC), free-light fraction (FLF), occluded-light fraction (OLF), and dense fraction (DF).

ers, primarily thought to be plant derived, had consistently older ^{14}C ages than bulk soil (Van Der Voort et al., 2017). Short-chain lipids, which can be microbial or root derived (Rethemeyer et al., 2004), were found to be younger than long-chain lipids throughout the soil profiles and younger than bulk soil at depth (Van Der Voort et al., 2017). However, microbial cell wall lipid biomarkers (glycerol dialkyl glycerol tetraethers, GDGTs) had older ^{14}C ages than bulk soils (Gies et al., 2021). With this consideration, our result regarding the more enriched ^{14}C of the TLE could be an indication of a predominance of short-chain lipids and suggested higher abundance of microbially derived lipids than plant-derived lipids. However, further study of specific lipid abundances (e.g., *n*-alkanes, fatty acids) in these soils is necessary as it is unclear to what degree lipids are older than bulk soils with depth because of preservation of these compounds through

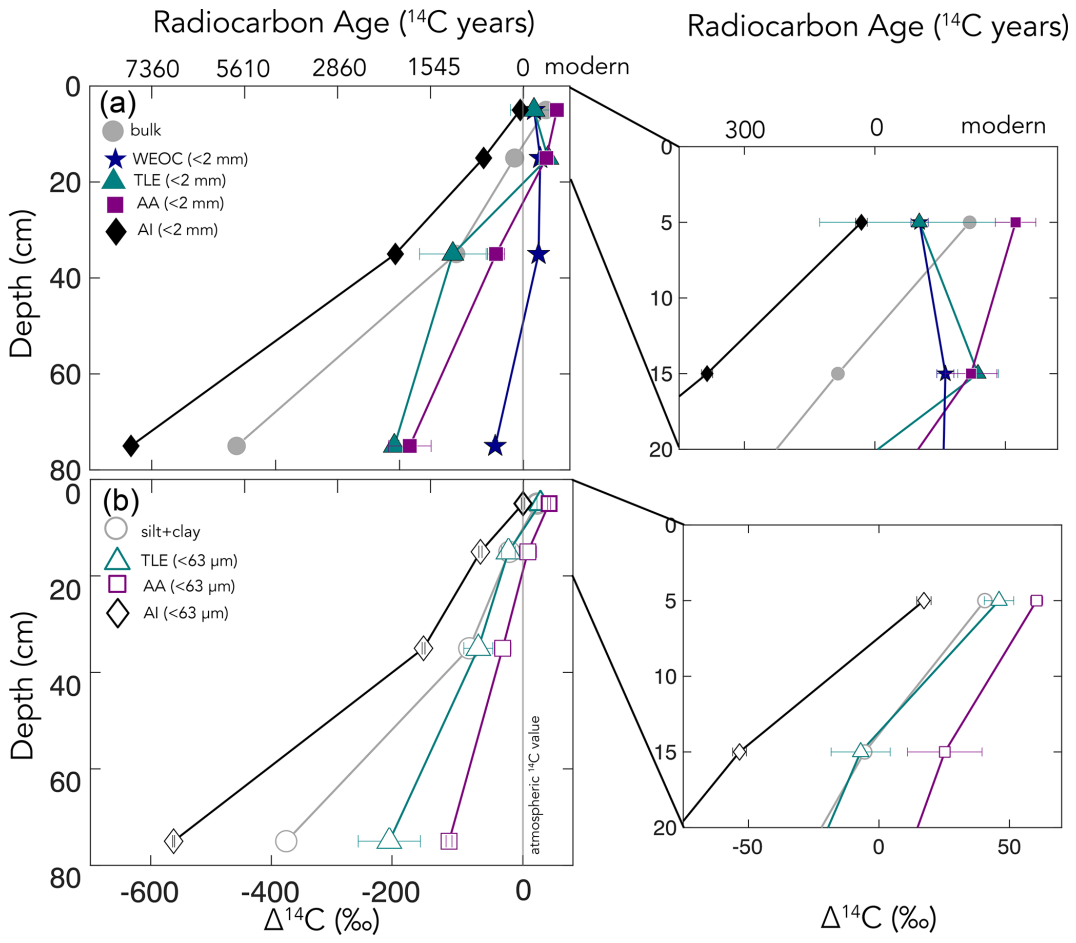

Figure 3. (a) Δ^{14}C by depth for bulk soil and four compound class fractions extracted from bulk soil for the entire depth profile, with the inset of the top 20 cm. **(b)** Δ^{14}C by depth for the silt + clay (< 63 µm) fraction and three compound classes extracted from the silt + clay for the entire depth profile, with the inset of the top 20 cm. For total lipid extract (TLE) and amino acid (AA) fractions ($n = 2$), error bars represent the standard error from duplicate measurements. For the < 2 mm, water extractable organic carbon (WEOC), and acid-insoluble (AI) fractions ($n = 1$), error bars represent analytical error. Error bars are smaller than the marker width where not shown.

mineral association or because of microbial use of aged-OC sources for growth.

We found that AI, the residual sample after both the TLEs and AAs have been extracted (Wang et al., 1998, 2006), was the most ^{14}C-depleted OC fraction measured at each soil depth (Figs. 3, 4) The AI fraction was far more depleted relative to the bulk soil (Figs. 3a and 4a) than observed in marine studies with acid-insoluble OC (Wang et al., 2006; Wang and Druffel, 2001). In these marine studies, the ^{14}C of the AI varied in age depending on the sampling depth and location. The significant depletion of the AI in our soils suggests that these chemically stable compounds are not oxidized in soil. Importantly, our AI samples are older than the other chemical and physical soil fractions that we measured in the soil, which is consistent with the general expectation that aromatic compounds can be difficult to degrade in soils (Ukalska-Jaruga et al., 2019).

4.2 Differential OC cycling between fractionation methods

Our results suggest different OC cycling timescales for the different physical fractions representing the "source" fractions. Here, we focus on the silt + clay fraction as an operationally defined mineral-associated OC pool. Numerous soil physical fractionation schemes have been applied to soils, and disparities in the methods challenge the interpretation and intercomparison of results from different studies using different approaches. We compared the size-based soil fractionation to the density fractionation to aid in the interpretation and comparability of our findings to other studies. Our silt + clay fraction had higher Δ^{14}C values than the sand, the POC-free sand, and the dense fraction (DF). Our silt + clay fraction could include free organic matter that passed through the 63 µm sieve but that would have floated off the DF during density fractionation. For reference, the free-light fraction

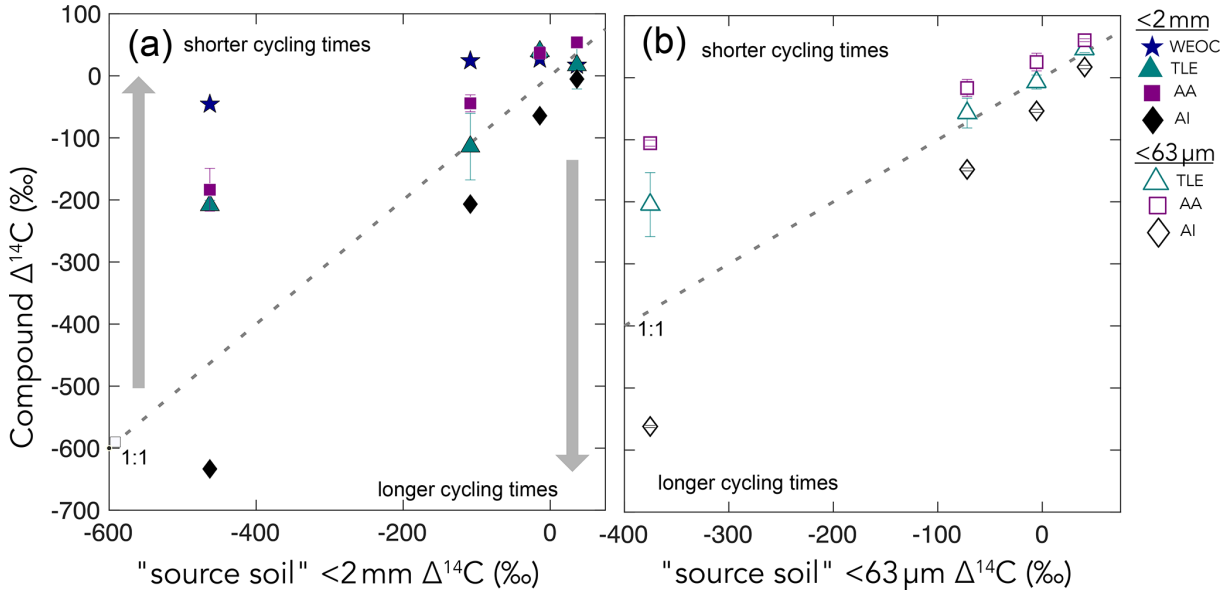

Figure 4. $\Delta^{14}C$ values of the four extracted compound classes – the water-extractable organic carbon (WEOC), the total lipid extract (TLE), the amino acid (AA) fraction, and the acid-insoluble (AI) fraction, (y axis) – compared to the $\Delta^{14}C$ values of the source soil or fraction (x axis) for **(a)** bulk soil and **(b)** silt + clay. The dashed gray lines show the 1 : 1 line where the bulk sample $\Delta^{14}C$ equals the compound class $\Delta^{14}C$. Gray arrows point to regions where data plot above or below the 1 : 1 line, suggesting that a given compound class has shorter and longer carbon turnover times than bulk soil, respectively.

(FLF) has higher $\Delta^{14}C$ values than the mineral-associated pools and bulk soils (Fig. 5) but also has high C/N, reflecting the high OC content and dominant plant origin of this fraction (Table S1). We assume that this small-size free OC is a small fraction of the total silt + clay OC as no small fragments of organic matter were visible and because the C/N ratios of the silt + clay fractions are only slightly elevated compared to the bulk soil and sand fractions (Table S1). Rather, the silt + clay fractions may have higher $\Delta^{14}C$ values relative to the POC-free sand and bulk soil because higher surface area in the silt + clay may facilitate mineral association with surface-derived OC (e.g., from the WEOC fraction).

Additionally, our TLE comparison between different size and density fractions highlights the important influence that method selection has over experimental results. Across studies, the mineral-associated OC is not a uniformly defined pool, and the observed results are a consequence of the methodology used to separate the samples (Fig. 6). The mineral-associated TLE cycled more rapidly than the bulk soil no matter which "mineral-associated" fraction (the silt + clay or the dense fraction) was chosen (Fig. 6). The $\Delta^{14}C$ values of TLE from the bulk, sand, and silt + clay fractions were indistinguishable from one another, possibly because the size fractionation scheme did not effectively separate distinct lipid pools. However, the $\Delta^{14}C$ values of TLE from the DF were significantly more ^{14}C-depleted than TLE from the silt + clay size fraction (Fig. 6), suggesting that there were older lipids in the DF relative to the silt + clay. However, more depleted ^{14}C values found in the TLE from the DF compared to the silt + clay could have resulted from the DF being exposed to SPT and/or ground after drying and before lipid extraction. It is possible that grinding the DF prior to lipid extraction increased the exposed surface area and resulted in a larger fraction of old SOC or rock-derived OC being incorporated into the TLE than if the DF had not been ground. We hesitate to definitively choose the best method for fractionation because each soil environment and experiment requires careful methodological consideration and selection. However, given the clear differences in results between mineral-associated organic matter (MAOM) derived from size and density fractionation, it appears that grinding the samples prior to extraction had significant effects on the age of the resulting TLE. Clearly, the approach used to fractionate soils influences experimental results and must be considered when interpreting differences in persistence across operationally defined OC pools.

4.3 Variation in OC cycling throughout the depth profile

The WEOC (extracted from bulk soils) and POC ($< 1\,g\,mL^{-1}$ floated off the sand size fraction) had the highest $\Delta^{14}C$ values throughout the soil profile, reflecting a predominance of modern carbon from plant detritus and root exudates to these pools. WEOC fractions can comprise a complex mixture of molecules with different structures (Hagedorn et al., 2004; Bahureksa et al., 2021), which are common only in their ability to be mobilized and dissolved

in water. WEOC can mobilize and percolate down the soil profile with sufficient precipitation to allow vertical transport. Both the POC and WEOC fractions supply OC that is readily accessible for microbial degradation and microbial utilization – resulting in the rapid turnover and relatively high $\Delta^{14}C$ values of these two pools (Marin-Spiotta et al., 2011). Occurrence of young OC in deep soils may be driven by microbial uptake of this young and bioavailable DOC or POC. Additionally, we found that the free-light density fractions were depleted in ^{14}C relative to the WEOC and POC (Fig. 5). We suspect that this is due to colloidal particles in the FLF, which are not dispersed or dense enough to settle in the SPT.

The study site has a Mediterranean climate, and these soils undergo seasonal wetting and drying cycles that may intensify in the future (Swain et al., 2018), potentially shifting the composition or amount of OC that percolates down the soil column, which could shift the age of the OC that the microbial community accesses at depth. Deeper in the soil profile, a greater reactive mineral surface area and lower microbial activity can enhance carbon stabilization in subsoils (Homyak et al., 2018; Dwivedi et al., 2017; Pries et al., 2023). Further research is needed to understand the effects of seasonal wetting and drying on the behavior of water-soluble OC in the soil profile.

In general, the $\Delta^{14}C$ values of the TLE, AA, and AI fractions decreased with increasing depth in the profile. While all extracted compounds followed this trend, the degree of ^{14}C depletion with depth varied somewhat between the different compound classes and between the bulk and silt + clay source fractions. The TLE extracted from the bulk and from the silt + clay fraction had similar slopes with depth. This suggests that depth has more influence than fraction size on resulting lipid ^{14}C content, possibly because of limited transport of lipids down the soil profile. The AAs extracted from the bulk and from the silt + clay fraction differed from one another in that the AAs extracted from the bulk soil became more depleted with depth than the AAs extracted from the silt + clay. This suggests that, at depth, AAs from the silt + clay fraction cycle more quickly than AAs extracted from the bulk soil, possibly indicating that the silt + clay fraction is more directly influenced by microbial activity than the sand fraction. At depths greater than 30 cm, the TLE and AA fraction were markedly younger than the bulk soil, possibly resulting from transport of lipids and amino acids from surface horizons down the profile; rapid recycling of these compounds at depth, the use of a relatively modern C source for lipid and amino acid synthesis at depth; or, most likely, a combination of these. At all depths the AI was significantly older than the source fraction, indicating that, throughout the soil profile, the AI contains an old and stable pool of OC.

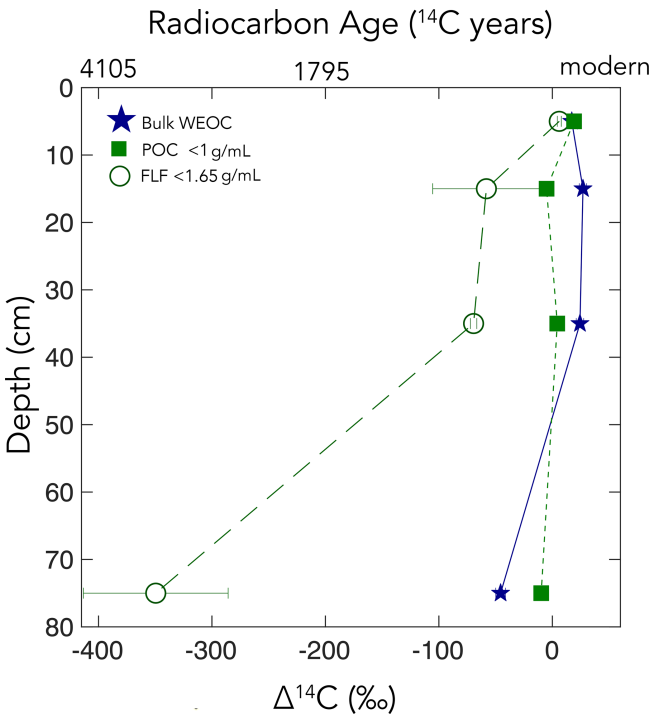

Figure 5. Particulate organic carbon (POC) (floated from the sand, $n = 1$), free-light fraction (FLF) (from bulk soil, $n = 3$, with error bars indicating the standard error of the mean), and water-extractable organic carbon (WEOC) (from bulk soil, $n = 1$). $\Delta^{14}C$ values by depth. For POC and WEOC, error bars indicating analytical error are generally smaller than the symbols.

4.4 Compound class $\Delta^{14}C$ values in mineral-associated SOC

To investigate the effect of mineral interaction on the $\Delta^{14}C$ values or the persistence of the TLE, AA, and AI, we measured these extracted compound classes from physical fractions intended to yield approximate mineral-associated carbon pools. We focused primarily on the silt + clay size fraction as the physical fraction that best approximates a mineral-associated OC pool derived from microbially processed plant inputs (Poeplau et al., 2018; Lavallee et al., 2020) and assume that, after size fractionation, most of the free organic matter in the bulk soil was in the sand size fraction. We compared the silt + clay size fraction $\Delta^{14}C$ values to the bulk $\Delta^{14}C$ values to determine if the material extracted from the isolated mineral-associated fractions of the soil had greater OC persistence or if these compounds cycled indiscriminately in relation to mineral association (Fig. 2).

While the TLE from the silt + clay and bulk soil had similar $\Delta^{14}C$ values, the AA from the silt + clay size fraction was enriched in ^{14}C compared to the AA from bulk soil ($r^2 = 0.98$, $p < 0.05$). This suggests that AAs cycle faster in the silt + clay mineral pool than in the bulk soils. While mineral surfaces usually are thought to promote stability and

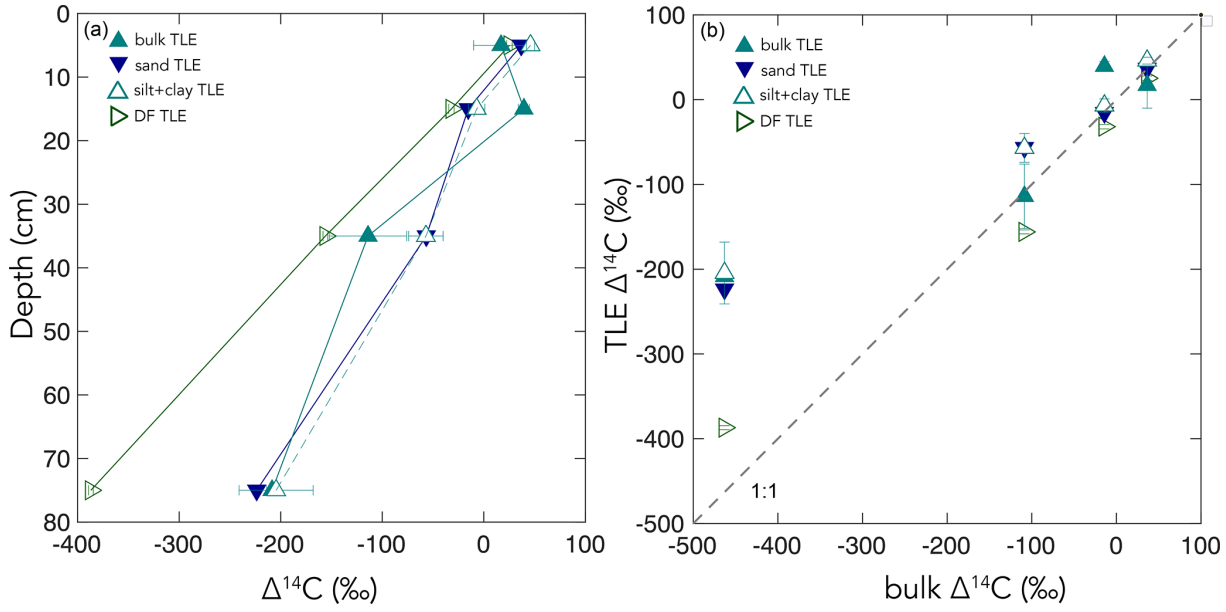

Figure 6. (a) $\Delta^{14}C$ versus soil depth measured for total lipid extractions (TLEs) from four soil size and/or density fractions, the bulk (< 2 mm), sand (63 µm to 2 mm), and dense fraction (DF). **(b)** A comparison of the bulk soil $\Delta^{14}C$ values to the TLEs from the four size and/or density fractions.

persistence of OC, in some soil systems, mineral associations may not be the single defining factor of OC persistence (Rocci et al., 2021) and could have a more nuanced role in influencing OC cycling in soils.

Our data suggest that there is a continuum of compounds that exist with different ^{14}C values in the mineral-associated pool because, in the silt + clay fraction, the TLEs, AAs, and AI have significantly different ^{14}C values (Fig. 4b). For instance, the mineral-associated TLE and AA fractions are enriched in ^{14}C relative to the silt + clay fraction, suggesting that both are cycling faster than the average mineral-associated pool. However, the AI from the silt + clay fraction cycles slower than the solid sample it was extracted from, and when we compare the AI from the bulk soil to the AI from the silt + clay, the AI from the silt + clay is slightly more ^{14}C-enriched. This suggests that there is slight ^{14}C enrichment across compounds in the silt + clay fraction relative to sand and bulk soil.

Our data suggest that lipids in mineral-associated OC pools vary in terms of cycling rates. This is complementary to findings from other studies where ^{14}C values from different lipid biomarkers are divergent from the bulk soils (Gies et al., 2021) and indicates the necessity of looking at entire compound class pools for understanding soil carbon persistence. Further investigation into the composition and age distribution of compounds within mineral-associated OC is needed to better quantify the distribution of cycling rates within mineral-associated OC pools.

4.5 Persistent and petrogenic OC

The most persistent, oldest OC was found in the AI fraction. Because carbon in the AI cycles more slowly than other components of this grassland soil, it is important to understand what structural components make up the AI and where these compounds are sourced from. Historically, the chemical structure of the AI fraction has been difficult to characterize. Hwang and Druffel (2003) argued that the AI is a lipid-like portion of the ocean OC. However, in soils, the AI can be composed of a mixture of lipid-like compounds and aromatic compounds (Silveira et al., 2008). In our soil, the ^{13}C–NMR spectra of the AI from 0 to 10 cm depth show a significant, broad peak in the 100–165 ppm range, indicative of aromatics (Fig. S3) (Baldock and Preston, 1995; Baldock et al., 1997). While it is possible that some condensed aromatic compounds form during the hydrolysis procedure used to remove AAs, the AI may also contain naturally occurring aromatic compounds that could include pyrogenic or petrogenic OC.

The parent material of our site is a mixture of sandstone, shale, greywacke, and schist (Foley et al., 2022); thus, it is possible that some of the OC in our soils is ancient, rock-derived, petrogenic carbon that has been incorporated into the soil profile through pedogenesis processes (Grant et al., 2023). Comparison of the AI to the rock (> 2 mm) fraction shows that the AI is younger than the OC contained in the rock fraction (Table S1), with the rock fraction $\Delta^{14}C$ values ranging from −481 ‰ to −765 ‰. To calculate the contribution of OC_{petro} to the AI fraction, we used a binary mixing

model with endmembers of OC_{petro} and aged SOC based on the method in Grant et al. (2023). The $\Delta^{14}C$ value of the $OC^{14}_{petro}C$ endmember is $-1000\,‰$, which is, by definition, ^{14}C-free, and the $\Delta^{14}C$ value of the biospheric endmember was set as either the measured TLE $\Delta^{14}C$ value or the bulk $\Delta^{14}C$ value from each depth. This comparison of these two different biospheric endmembers allowed us to calculate a possible range of values for the OC_{petro} contribution (Table 1). In the AI extracted from the silt + clay fraction, the OC_{petro} contribution was 4 %–5 % from 0 to 10 cm depth and 40 %–53 % in the 50–100 cm depth range. In AI extracted from the bulk soil, the OC_{petro} contribution was 0 %–1 % in the 0–10 cm depth range and 17 %–44 % in the 50–100 cm depth range. Therefore, while the AI fraction likely contains OC_{petro}, it is primarily composed of OC compounds derived from more recent plant and microbial inputs that are highly resistant to acid hydrolysis either because of their chemical structure or because of their strong associations with minerals.

5 Conclusions and continued soil radiocarbon compound class characterization

In this study, we characterized a soil carbon profile using compound class ^{14}C analyses. We found that our extraction methods yielded fractions with ^{14}C signatures that are distinctly different from those of the source soil from which they were extracted. We found that, in this annual grassland soil, the AA and the TLE fractions cycle more rapidly than the bulk soil throughout the soil profile. At each depth, the AI fraction is the oldest fraction and contains a combination of slow-cycling SOC and ancient petrogenic C. These results show that soil compound classes cycle differently than similar components in marine systems. Our results also show that mineral-associated SOC contains a mixture of carbon compounds with distinctly different ages and sources that drive turnover and persistence. Compound-specific ^{14}C approaches hold promise for improving our understanding of the chemical structure of SOC, as well as of the connection between carbon degradation and preservation in soils. A molecule-resolved understanding of the relationship between compound classes and carbon persistence will also give insight into the fate and turnover time of specific organic biomarkers found in plant residues or the biomass of bacteria, fungi, and microfauna. These techniques can also help to determine mechanisms promoting mineral stabilization of soil carbon, especially when combined with soil physical fractionation.

Results from this study highlight that radiocarbon measurements of specific organic compounds and compound classes in soil provide valuable insights into the persistence and decomposition rates of soil organic carbon. To improve our ability to model the future of soil carbon stocks and soil quality in the face of a changing global climate, we need further research that interrogates the composition, radiocarbon content, and cycling rates of soil organic carbon and that mechanistically links these rates to physical and chemical drivers.

Data availability. A list of all radiocarbon data, stable carbon, and total OC values, with a CAMS tracking number for each of the analyses used in this publication, can be found in the Supplement below.

Supplement. The supplement related to this article is available online at: https://doi.org/10.5194/bg-21-4395-2024-supplement.

Author contributions. KJM, KMF, TABB, JP, and KEG conceptualized the study. KJM, KMF, TABB, and JP secured funding for the project. KEG designed the method and carried out the extractions with input from KJM, KMF, and TABB. CJL carried out the density separations. MNR carried out the water extractions. JDK and MM ran the NMR experiments. KEG, KJM, and KMF interpreted the data. KEG prepared the paper with the contributions of all the co-authors.

Competing interests. The contact author has declared that none of the authors has any competing interests.

Disclaimer. Publisher's note: Copernicus Publications remains neutral with regard to jurisdictional claims made in the text, published maps, institutional affiliations, or any other geographical representation in this paper. While Copernicus Publications makes every effort to include appropriate place names, the final responsibility lies with the authors.

Acknowledgements. This work was performed under the auspices of the US Department of Energy by Lawrence Livermore National Laboratory under contract no. DE-AC52-07NA27344 and IM tracking no. LLNL-JRNL-843138. Additional support with regard to site access, sample collection, and site characterization data was provided by the US Department of Energy, Office of Biological and Environmental Research, Genomic Sciences Program LLNL "Microbes Persist" Scientific Focus Area (award no. SCW1632). We acknowledge the traditional, ancestral, unceded territory of the Shóqowa and Hopland people, on which this research was conducted. We thank the staff at the Hopland Research and Extension Center who manage the experiment site, and we thank Z Kagely for his assistance in digging the soil pit.

Financial support. This research has been supported by the LLNL LDRD Program under project nos. 21-ERD-021 and 24-SI-002. Additional support was provided by the US Department of Energy, Office of Biological and Environmental Research, Genomic Science program LLNL "Microbes Persist" Scientific Focus Area (award no. SCW1632).

Review statement. This paper was edited by Cindy De Jonge and reviewed by Rienk Smittenberg and one anonymous referee.

References

Agnelli, A., Trumbore, S. E., Corti, G., and Ugolini, F. C.: The dynamics of organic matter in rock fragments in soil investigated by ^{14}C dating and measurements of ^{13}C, Europ. J. Soil Sci., 53, 147–159, https://doi.org/10.1046/j.1365-2389.2002.00432.x, 2002.

Angst, G., John, S., Mueller, C. W., Kögel-Knabner, I., and Rethemeyer, J.: Tracing the sources and spatial distribution of organic carbon in subsoils using a multi-biomarker approach, Sci. Rep., 6, 1–12, 2016.

Angst, G., Mueller, K. E., Nierop, K. G. J., and Simpson, M. J.: Plant- or microbial-derived? A review on the molecular composition of stabilized soil organic matter, Soil Biol. Biochem., 156, 108189, https://doi.org/10.1016/j.soilbio.2021.108189, 2021.

Bahureksa, W., Tfaily, M. M., Boiteau, R. M., Young, R. B., Logan, M. N., McKenna, A. M., and Borch, T.: Soil Organic Matter Characterization by Fourier Transform Ion Cyclotron Resonance Mass Spectrometry (FTICR MS): A Critical Review of Sample Preparation, Analysis, and Data Interpretation, Environ. Sci. Technol., 55, 9637–9656, https://doi.org/10.1021/acs.est.1c01135, 2021.

Baldock, J. A. and Preston, C. M.: Chemistry of Carbon Decomposition Processes in Forests as Revealed by Solid-State Carbon-13 Nuclear Magnetic Resonance, Carbon Forms and Functions in Forest Soils, 89–117, https://doi.org/10.2136/1995.carbonforms.c6, 1995.

Baldock, J. A., Oades, J. M., Nelson, P. N., Skene, T. M., Golchin, A., and Clarke, P.: Assessing the extent of decomposition of natural organic materials using solid-state ^{13}C NMR spectroscopy, Soil Res., 35, 1061–1084, https://doi.org/10.1071/S97004, 1997.

Bartolome, J. W., James Barry, W., Griggs, T., and Hopkinson, P.: Valley Grassland, in: Terrestrial Vegetation of California, edited by: Barbour, M., University of California Press, https://doi.org/10.1525/california/9780520249554.003.0014, 2007.

Blattmann, T. M., Montluçon, D. B., Haghipour, N., Ishikawa, N. F., and Eglinton, T. I.: Liquid Chromatographic Isolation of Individual Amino Acids Extracted From Sediments for Radiocarbon Analysis, Front. Mar. Sci., 7, 174, https://doi.org/10.3389/fmars.2020.00174, 2020.

Bour, A. L., Walker, B. D., Broek, T. A. B., and McCarthy, M. D.: Radiocarbon Analysis of Individual Amino Acids: Carbon Blank Quantification for a Small-Sample High-Pressure Liquid Chromatography Purification Method, Anal. Chem., 88, 3521–3528, https://doi.org/10.1021/acs.analchem.5b03619, 2016.

Broek, T. A. B., Ognibene, T. J., McFarlane, K. J., Moreland, K. C., Brown, T. A., and Bench, G.: Conversion of the LLNL/-CAMS 1 MV biomedical AMS system to a semi-automated natural abundance ^{14}C spectrometer: system optimization and performance evaluation, Nucl. Instrum. Meth. B, 499, 124–132, https://doi.org/10.1016/j.nimb.2021.01.022, 2021.

Coppola, A. I., Wiedemeier, D. B., Galy, V., Haghipour, N., Hanke, U. M., Nascimento, G. S., Usman, M., Blattmann, T. M., Reisser, M., Freymond, C. V., Zhao, M., Voss, B., Wacker, L., Schefuß, E., Peucker-Ehrenbrink, B., Abiven, S., Schmidt, M. W. I., and Eglinton, T. I.: Global-scale evidence for the refractory nature of riverine black carbon, Nat. Geosci., 11, 584–588, https://doi.org/10.1038/s41561-018-0159-8, 2018.

De Troyer, I., Amery, F., Van Moorleghem, C., Smolders, E., and Merckx, R.: Tracing the source and fate of dissolved organic matter in soil after incorporation of a ^{13}C labelled residue: A batch incubation study, Soil Biol. Biochem., 43, 513–519, https://doi.org/10.1016/j.soilbio.2010.11.016, 2011.

Douglas, P. M. J., Pagani, M., Eglinton, T. I., Brenner, M., Curtis, J. H., Breckenridge, A., and Johnston, K.: A long-term decrease in the persistence of soil carbon caused by ancient Maya land use, Nat. Geosci., 11, 645–649, https://doi.org/10.1038/s41561-018-0192-7, 2018.

Dwivedi, D., Riley, W., Torn, M., Spycher, N., Maggi, F., and Tang, J.: Mineral properties, microbes, transport, and plant-input profiles control vertical distribution and age of soil carbon stocks, Soil Biol. Biochem., 107, 244–259, 2017.

Eglinton, T. I., Galy, V. V., Hemingway, J. D., Feng, X., Bao, H., Blattmann, T. M., Dickens, A. F., Gies, H., Giosan, L., Haghipour, N., Hou, P., Lupker, M., McIntyre, C. P., Montlucon, D. B., Peucker-Ehrenbrink, B., Ponton, C., Schefuss, E., Schwab, M. S., Voss, B. M., Wacker, L., Wu, Y., and Zhao, M.: Climate control on terrestrial biospheric carbon turnover, P. Natl. Acad. Sci. USA, 118, e2011585118, https://doi.org/10.1073/pnas.2011585118, 2021.

Feng, X., Benitez-Nelson, B. C., Montluçon, D. B., Prahl, F. G., McNichol, A. P., Xu, L., Repeta, D. J., and Eglinton, T. I.: ^{14}C and ^{13}C characteristics of higher plant biomarkers in Washington margin surface sediments, Geochim. Cosmochim. Ac., 105, 14–30, https://doi.org/10.1016/j.gca.2012.11.034, 2013.

Feng, X., Vonk, J. E., Griffin, C., Zimov, N., Montluçon, D. B., Wacker, L., and Eglinton, T. I.: ^{14}C Variation of Dissolved Lignin in Arctic River Systems, ACS Earth Space Chem., 1, 334–344, https://doi.org/10.1021/acsearthspacechem.7b00055, 2017.

Finstad, K. M., Nuccio, E. E., Grant, K. E., Broek, T. A. B., Pett-Ridge, J., and McFarlane, K. J.: Radiocarbon analysis of soil microbial biomass via direct chloroform extraction, Radiocarbon, 1–9, https://doi.org/10.1017/RDC.2023.80, 2023.

Foley, M. M., Blazewicz, S. J., McFarlane, K. J., Greenlon, A., Hayer, M., Kimbrel, J. A., Koch, B. J., Monsaint-Queeney, V., Morrison, K., Morrissey, E., Hungate, B. A., and Pett-Ridge, J.: Active populations and growth of soil microorganisms are framed by mean annual precipitation in three California annual grasslands, Soil Biol. Biochem., 177, 108886, https://doi.org/10.1016/j.soilbio.2022.108886, 2022.

Galy, V., Beyssac, O., France-Lanord, C., and Eglinton, T.: Recycling of Graphite During Himalayan Erosion: A Geological Stabilization of Carbon in the Crust, Science, 322, 943–945, https://doi.org/10.1126/science.1161408, 2008.

Galy, V., Peucker-Ehrenbrink, B., and Eglinton, T.: Global carbon export from the terrestrial biosphere controlled by erosion, Nature, 521, 204–207, https://doi.org/10.1038/nature14400, 2015.

Gaudinski, J. B., Trumbore, S. E., Davidson, E. A., and Zheng, S.: Soil carbon cycling in a temperate forest: radiocarbon-based estimates of residence times, sequestration rates and partitioning of fluxes, Biogeochemistry, 51, 33–69, https://doi.org/10.1023/A:1006301010014, 2000.

Gies, H., Hagedorn, F., Lupker, M., Montluçon, D., Haghipour, N., van der Voort, T. S., and Eglinton, T. I.: Millennial-age glycerol dialkyl glycerol tetraethers (GDGTs) in forested mineral soils: ^{14}C-based evidence for stabilization of microbial necromass, Biogeosciences, 18, 189–205, https://doi.org/10.5194/bg-18-189-2021, 2021.

Gleixner, G.: Soil organic matter dynamics: a biological perspective derived from the use of compound-specific isotopes studies, Ecol. Res., 28, 683–695, 2013.

Grant, K. E., Galy, V. V., Haghipour, N., Eglinton, T. I., and Derry, L. A.: Persistence of old soil carbon under changing climate: The role of mineral-organic matter interactions, Chem. Geol., 587, 120629, https://doi.org/10.1016/j.chemgeo.2021.120629, 2022.

Grant, K. E., Hilton, R. G., and Galy, V. V.: Global patterns of radiocarbon depletion in subsoil linked to rock-derived organic carbon, Geochem. Perspect. Lett., 25, 36–40, https://doi.org/10.7185/geochemlet.2312, 2023.

Hagedorn, F., Saurer, M., and Blaser, P.: A ^{13}C tracer study to identify the origin of dissolved organic carbon in forested mineral soils, Europ. J. Soil Sci., 55, 91–100, https://doi.org/10.1046/j.1365-2389.2003.00578.x, 2004.

Hein, C. J., Usman, M., Eglinton, T. I., Haghipour, N., and Galy, V. V.: Millennial-scale hydroclimate control of tropical soil carbon storage, Nature, 581, 63–66, https://doi.org/10.1038/s41586-020-2233-9, 2020.

Homyak, P. M., Blankinship, J. C., Slessarev, E. W., Schaeffer, S. M., Manzoni, S., and Schimel, J. P.: Effects of altered dry season length and plant inputs on soluble soil carbon, Ecology, 99, 2348–2362, https://doi.org/10.1002/ecy.2473, 2018.

Hua, Q., Turnbull, J. C., Santos, G. M., Rakowski, A. Z., Ancapichún, S., De Pol-Holz, R., Hammer, S., Lehman, S. J., Levin, I., Miller, J. B., Palmer, J. G., and Turney, C. S. M.: Atmospheric Radiocarbon For The Period 1950–2019, Radiocarbon, 64, 723–745, https://doi.org/10.1017/RDC.2021.95, 2022.

Huang, Y., Bol, R., Harkness, D. D., Ineson, P., and Eglinton, G.: Post-glacial variations in distributions, ^{13}C and ^{14}C contents of aliphatic hydrocarbons and bulk organic matter in three types of British acid upland soils, Org. Geochem., 24, 273–287, https://doi.org/10.1016/0146-6380(96)00039-3, 1996.

Hwang, J. and Druffel, E. R. M.: Lipid-Like Material as the Source of the Uncharacterized Organic Carbon in the Ocean?, Science, 299, 881–884, https://doi.org/10.1126/science.1078508, 2003.

Ishikawa, N. F., Itahashi, Y., Blattmann, T. M., Takano, Y., Ogawa, N. O., Yamane, M., Yokoyama, Y., Nagata, T., Yoneda, M., Haghipour, N., Eglinton, T. I., and Ohkouchi, N.: Improved Method for Isolation and Purification of Underivatized Amino Acids for Radiocarbon Analysis, Anal. Chem., 90, 12035–12041, https://doi.org/10.1021/acs.analchem.8b02693, 2018.

Jia, J., Liu, Z., Haghipour, N., Wacker, L., Zhang, H., Sierra, C. A., Ma, T., Wang, Y., Chen, L., Luo, A., Wang, Z., He, J.-S., Zhao, M., Eglinton, T. I., and Feng, X.: Molecular ^{14}C evidence for contrasting turnover and temperature sensitivity of soil organic matter components, Ecol. Lett., 26, 778–788, https://doi.org/10.1111/ele.14204, 2023.

Jobbágy, E. G. and Jackson, R. B.: The vertical distribution of soil organic carbon and its relation to climate and vegetation, Ecol. Appl., 10, 423–436, https://doi.org/10.1890/1051-0761(2000)010[0423:TVDOSO]2.0.CO;2, 2000.

Keiluweit, M., Bougoure, J. J., Nico, P. S., Pett-Ridge, J., Weber, P. K., and Kleber, M.: Mineral protection of soil carbon counteracted by root exudates, Nat. Clim. Change, 5, 588–595, 2015.

Kleber, M., Sollins, P., and Sutton, R.: A conceptual model of organo-mineral interactions in soils: self-assembly of organic molecular fragments into zonal structures on mineral surfaces, Biogeochemistry, 85, 9–24, 2007.

Kleber, M., Bourg, I. C., Coward, E. K., Hansel, C. M., Myneni, S. C. B., and Nunan, N.: Dynamic interactions at the mineral–organic matter interface, Nat. Rev. Earth Environ., 2, 402–421, 2021.

Kögel-Knabner, I.: The macromolecular organic composition of plant and microbial residues as inputs to soil organic matter, Soil Biol. Biochem., 34, 139–162, https://doi.org/10.1016/S0038-0717(01)00158-4, 2002.

Kotanen, P. M.: Revegetation following Soil Disturbance and Invasion in a Californian Meadow: a 10-year History of Recovery, Biol. Invasions, 6, 245–254, https://doi.org/10.1023/B:BINV.0000022145.03215.4f, 2004.

Kuzyakov, Y., Bogomolova, I., and Glaser, B.: Biochar stability in soil: Decomposition during eight years and transformation as assessed by compound-specific ^{14}C analysis, Soil Biol. Biochem., 70, 229–236, https://doi.org/10.1016/j.soilbio.2013.12.021, 2014.

Lavallee, J. M., Soong, J. L., and Cotrufo, M. F.: Conceptualizing soil organic matter into particulate and mineral-associated forms to address global change in the 21st century, Glob. Change Biol., 26, 261–273, https://doi.org/10.1111/gcb.14859, 2020.

Lechleitner, F. A., Baldini, J. U. L., Breitenbach, S. F. M., Fohlmeister, J., McIntyre, C., Goswami, B., Jamieson, R. A., van der Voort, T. S., Prufer, K., Marwan, N., Culleton, B. J., Kennett, D. J., Asmerom, Y., Polyak, V., and Eglinton, T. I.: Hydrological and climatological controls on radiocarbon concentrations in a tropical stalagmite, Geochim. Cosmochim. Ac., 194, 233–252, https://doi.org/10.1016/j.gca.2016.08.039, 2016.

Lehmann, J. and Kleber, M.: The contentious nature of soil organic matter, Nature, 528, 60–68, https://doi.org/10.1038/nature16069, 2015.

Lehmann, J., Hansel, C. M., Kaiser, C., Kleber, M., Maher, K., Manzoni, S., Nunan, N., Reichstein, M., Schimel, J. P., Torn, M. S., Wieder, W. R., and Kögel-Knabner, I.: Persistence of soil organic carbon caused by functional complexity, Nat. Geosci., 13, 529–534, https://doi.org/10.1038/s41561-020-0612-3, 2020.

Levin, I. and Hesshaimer, V.: Radiocarbon – A Unique Tracer of Global Carbon Cycle Dynamics, Radiocarbon, 42, 69–80, 2000.

Loh, A. N., Bauer, J. E., and Druffel, E. R. M.: Variable ageing and storage of dissolved organic components in the open ocean, Nature, 430, 877–881, https://doi.org/10.1038/nature02780, 2004.

Lützow, M. v., Kögel-Knabner, I., Ekschmitt, K., Matzner, E., Guggenberger, G., Marschner, B., and Flessa, H.: Stabilization of organic matter in temperate soils: mechanisms and their relevance under different soil conditions – a review, Europ. J. Soil Sci., 57, 426–445, https://doi.org/10.1111/j.1365-2389.2006.00809.x, 2006.

Marin-Spiotta, E., Chadwick, O. A., Kramer, M., and Carbone, M. S.: Carbon delivery to deep mineral horizons in Hawaiian rain forest soils, J. Geophys. Res.-Biogeo., 116, G03011, https://doi.org/10.1029/2010JG001587, 2011.

McFarlane, K. J., Torn, M. S., Hanson, P. J., Porras, R. C., Swanston, C. W., Callaham, M. A., and Guilderson, T. P.: Comparison of soil organic matter dynamics at five temperate deciduous forests with physical fractionation and radiocarbon measurements, Biogeochemistry, 112, 457–476, https://doi.org/10.1007/s10533-012-9740-1, 2013.

Mikutta, R., Mikutta, C., Kalbitz, K., Scheel, T., Kaiser, K., and Jahn, R.: Biodegradation of forest floor organic matter bound to minerals via different binding mechanisms, Geochim. Cosmochim. Ac., 71, 2569–2590, 2007.

Moe, L. A.: Amino acids in the rhizosphere: From plants to microbes, Am. J. Bot., 100, 1692–1705, https://doi.org/10.3732/ajb.1300033, 2013.

Nuccio, E. E., Anderson-Furgeson, J., Estera, K. Y., Pett-Ridge, J., De Valpine, P., Brodie, E. L., and Firestone, M. K.: Climate and edaphic controllers influence rhizosphere community assembly for a wild annual grass, Ecology, 97, 1307–1318, https://doi.org/10.1890/15-0882.1, 2016.

Poeplau, C., Don, A., Six, J., Kaiser, M., Benbi, D., Chenu, C., Cotrufo, M. F., Derrien, D., Gioacchini, P., Grand, S., Gregorich, E., Griepentrog, M., Gunina, A., Haddix, M., Kuzyakov, Y., Kühnel, A., Macdonald, L. M., Soong, J., Trigalet, S., Vermeire, M.-L., Rovira, P., van Wesemael, B., Wiesmeier, M., Yeasmin, S., Yevdokimov, I., and Nieder, R.: Isolating organic carbon fractions with varying turnover rates in temperate agricultural soils – A comprehensive method comparison, Soil Biol. Biochem., 125, 10–26, https://doi.org/10.1016/j.soilbio.2018.06.025, 2018.

Pries, C. E. H., Ryals, R., Zhu, B., Min, K., Cooper, A., Goldsmith, S., Pett-Ridge, J., Torn, M., and Berhe, A. A.: The Deep Soil Organic Carbon Response to Global Change, Annu. Rev. Ecol. Evol. S., 54, 375–401, https://doi.org/10.1146/annurev-ecolsys-102320-085332, 2023.

R Core Team: R: A language and environment for statistical computing, R Foundation for Statistical Computing [code], Vienna, Austria, https://www.R-project.org/ (last access: 10 November 2023), 2021.

Repasch, M., Scheingross, J. S., Hovius, N., Lupker, M., Wittmann, H., Haghipour, N., Gröcke, D. R., Orfeo, O., Eglinton, T. I., and Sachse, D.: Fluvial organic carbon cycling regulated by sediment transit time and mineral protection, Nat. Geosci., 14, 842–848, https://doi.org/10.1038/s41561-021-00845-7, 2021.

Rethemeyer, J., Kramer, C., Gleixner, G., Wiesenberg, G. L. B., Schwark, L., Andersen, N., Nadeau, M.-J., and Grootes, P. M.: Complexity of Soil Organic Matter: AMS ^{14}C Analysis of Soil Lipid Fractions and Individual Compounds, Radiocarbon, 46, 465–473, https://doi.org/10.1017/S0033822200039771, 2004.

Rocci, K. S., Lavallee, J. M., Stewart, C. E., and Cotrufo, M. F.: Soil organic carbon response to global environmental change depends on its distribution between mineral-associated and particulate organic matter: A meta-analysis, Sci. Total Environ., 793, 148569, https://doi.org/10.1016/j.scitotenv.2021.148569, 2021.

Schmidt, M. W., Torn, M. S., Abiven, S., Dittmar, T., Guggenberger, G., Janssens, I. A., Kleber, M., Kögel-Knabner, I., Lehmann, J., and Manning, D. A.: Persistence of soil organic matter as an ecosystem property, Nature, 478, 49–56, 2011.

Shi, Z., Allison, S. D., He, Y., Levine, P. A., Hoyt, A. M., Beem-Miller, J., Zhu, Q., Wieder, W. R., Trumbore, S., and Randerson, J. T.: The age distribution of global soil carbon inferred from radiocarbon measurements, Nat. Geosci., 13, 555–559, 2020.

Sierra, C. A., Müller, M., and Trumbore, S. E.: Modeling radiocarbon dynamics in soils: SoilR version 1.1, Geosci. Model Dev., 7, 1919–1931, https://doi.org/10.5194/gmd-7-1919-2014, 2014.

Silveira, M. L., Comerford, N. B., Reddy, K. R., Cooper, W. T., and El-Rifai, H.: Characterization of soil organic carbon pools by acid hydrolysis, Geoderma, 144, 405–414, https://doi.org/10.1016/j.geoderma.2008.01.002, 2008.

Smittenberg, R. H., Eglinton, T. I., Schouten, S., Damsté, J. S. S.: Ongoing Buildup of Refractory Organic Carbon in Boreal Soils During the Holocene, Science, 314, 1283–1286, 2006.

Soil Survey Staff: Keys to Soil Taxonomy, 13th Edn., USDA Natural Resources Conservation Service, 2022.

Stoner, S., Trumbore, S. E., González-Pérez, J. A., Schrumpf, M., Sierra, C. A., Hoyt, A. M., Chadwick, O., and Doetterl, S.: Relating mineral–organic matter stabilization mechanisms to carbon quality and age distributions using ramped thermal analysis, Philos. T. R. Soc. A, 381, 20230139, https://doi.org/10.1098/rsta.2023.0139, 2023.

Stuiver, M. and Polach, H. A.: Discussion Reporting of ^{14}C Data, Radiocarbon, 19, 355–363, https://doi.org/10.1017/s0033822200003672, 1977.

Swain, D. L., Langenbrunner, B., Neelin, J. D., and Hall, A.: Increasing precipitation volatility in twenty-first-century California, Nat. Clim. Change, 8, 427–433, https://doi.org/10.1038/s41558-018-0140-y, 2018.

Torn, M. S., Swanston, C. W., Castanha, C., and Trumbore, S. E.: Storage and Tunover of Organic Matter in Soil, in: Biophysico-Chemical Processes Involving Natural Nonliving Organic Matter in Environmental Systems, edited by: Senesi, N., Xing, B., and Huang, P. M., Wiley-IUPAC series in biopysico-chemical processes in environmental systems, John Wiley & Sons, Inc., Hoboken, New Jersey, 219–272, https://doi.org/10.1002/9780470494950.ch6, 2009.

Trumbore, S.: Age of Soil Organic Matter and Soil Respiration: Radiocarbon Constraints on Belowground C Dynamics, Ecol. Appl., 10, 399–411, https://doi.org/10.2307/2641102, 2000.

Trumbore, S. E. and Harden, J. W.: Accumulation and turnover of carbon in organic and mineral soils of the BOREAS northern study area, J. Geophys. Res.-Atmos., 102, 28817–28830, https://doi.org/10.1029/97jd02231, 1997.

Trumbore, S. E. and Zheng, S.: Comparison of Fractionation Methods for Soil Organic Matter 14C Analysis, Radiocarbon, 38, 219–229, https://doi.org/10.1017/s0033822200017598, 1996.

Ukalska-Jaruga, A., Smreczak, B., and Klimkowicz-Pawlas, A.: Soil organic matter composition as a factor affecting the accumulation of polycyclic aromatic hydrocarbons, J. Soil. Sediment., 19, 1890–1900, https://doi.org/10.1007/s11368-018-2214-x, 2019.

van der Voort, T. S., Zell, C. I., Hagedorn, F., Feng, X., McIntyre, C. P., Haghipour, N., Graf Pannatier, E., and Eglinton, T. I.: Diverse Soil Carbon Dynamics Expressed at the Molecular Level, Geophys. Res. Lett., 44, 11, 840–850, https://doi.org/10.1002/2017gl076188, 2017.

van der Voort, T. S., Mannu, U., Hagedorn, F., McIntyre, C., Walthert, L., Schleppi, P., Haghipour, N., and Eglinton, T. I.: Dynamics of deep soil carbon – insights from ^{14}C time series across a climatic gradient, Biogeosciences, 16, 3233–3246, https://doi.org/10.5194/bg-16-3233-2019, 2019.

Vogel, C., Mueller, C. W., Höschen, C., Buegger, F., Heister, K., Schulz, S., Schloter, M., and Kögel-Knabner, I.: Submicron structures provide preferential spots for carbon and nitrogen sequestration in soils, Nat. Commun., 5, 2947, https://doi.org/10.1038/ncomms3947, 2014.

Vogel, J. S., Southon, J. R., Nelson, D. E., and Brown, T. A.: Performance of catalytically condensed carbon for use in accelerator mass spectrometry, Nucl. Instrum. Meth. B, 5, 289–293, https://doi.org/10.1016/0168-583X(84)90529-9, 1984.

von Lutzow, M., Kogel-Knabner, I., Ekschmitt, K., Flessa, H., Guggenberger, G., Matzner, E., and Marschner, B.: SOM fractionation methods: Relevance to functional pools and to stabilization mechanisms, Soil Biol. Biochem., 39, 2183–2207, 2007.

Wang, X.-C. and Druffel, E. R. M.: Radiocarbon and stable carbon isotope compositions of organic compound classes in sediments from the NE Pacific and Southern Oceans, Mar. Chem., 73, 65–81, https://doi.org/10.1016/S0304-4203(00)00090-6, 2001.

Wang, X.-C., Druffel, E. R. M., Griffin, S., Lee, C., and Kashgarian, M.: Radiocarbon studies of organic compound classes in plankton and sediment of the northeastern Pacific Ocean, Geochim. Cosmochim. Ac., 62, 1365–1378, https://doi.org/10.1016/S0016-7037(98)00074-X, 1998.

Wang, X.-C., Callahan, J., and Chen, R. F.: Variability in radiocarbon ages of biochemical compound classes of high molecular weight dissolved organic matter in estuaries, Estuar. Coast. Shelf Sci., 68, 188–194, https://doi.org/10.1016/j.ecss.2006.01.018, 2006.